

Platinum Nanoparticles Supported on Carbon Nanodots as Anode Catalysts for Direct Alcohol Fuel Cells

S. S Gwebu¹, P.N Nomngongo¹, P.N Mashazi², T Nyokong², N.W Maxakato^{1,*}

¹ Department of Applied Chemistry, University of Johannesburg, Doornfontein, 2028, South Africa

² Chemistry Department, Rhodes University, Grahamstown, 6139, South Africa

*E-mail: nmaxakato@uj.ac.za

Received: 31 January 2017 / Accepted: 2 May 2017 / Published: 12 June 2017

Carbon nanodots (CNDs) were successfully synthesized employing a cheap and green method using oats as a starting material. The Pt/CNDs electrocatalyst was synthesized using carbon nanodots as a reductant and support material without adjusting the pH of the solution. The synthesized materials were characterized using Fourier transform infrared spectroscopy (FTIR), Brunauer-Emmett-Teller Nitrogen adsorption (BET), X-ray photoelectron spectroscopy (XPS), Transmission electron microscopy (TEM), X-ray diffractometry (XRD) and Inductively coupled plasma optical emission spectroscopy (ICP-OES). The FTIR results proved that the synthesized carbon nanodots contain carboxylic acid functional groups which facilitate the attachment of Pt nanoparticles. The BET surface area for carbon nanodots was found to be $312.5 \text{ m}^2\text{g}^{-1}$ two times higher than that of commercial carbon. XPS results revealed the composition of the materials and the oxidation states of Pt in Pt/CNDs electrocatalyst. TEM images proved that the materials were of the nanoscale. XRD peaks proved that the carbon nanodots were amorphous and Pt (111) was present in the Pt/CNDs electrocatalyst. ICP-OES determined the platinum concentration in Pt/CNDs electrocatalyst to be 8.12%. The electrochemical oxidation of methanol and ethanol were studied by cyclic voltammetry (CV) and chronoamperometry (CA). Cyclic voltammetry results showed that the Pt/CNDs electrocatalyst prepared by this method exhibit superior performance for methanol and ethanol electro-oxidation at room temperature.

Keywords: carbon nanodots; electrocatalyst; direct alcohol fuel cells; cyclic voltammetry; chronoamperometry; methanol; ethanol.

1. INTRODUCTION

Carbon possesses unique electrical and structural properties that make it an ideal material for use in fuel cell construction. Carbon nanodots (CNDs) are a new class of carbon nanomaterials with

particle sizes below 10 nm [1,2]. They generally possess a sp^2 conjugated core and contain suitable oxygen content in the form of multiple oxygen-containing functional groups such as carboxyl, hydroxyl and aldehyde. Synthesis of carbon nanodots can be classified into two main groups: Top down (chemical) and bottom up (physical) methods [3,4]. The top-down method employs treating starting materials such as graphite powder or multi-walled carbon nanotubes (MWCNTs) in harsh chemical conditions [4]. Bottom-up approach involves applying external energy such as ultrasonication [5], microwave pyrolysis [6] and hydrothermal treatment of small molecules such as starch [7], citric acid [8] glucose [5] and leeks [9]. CNDs have widely been applied in bioimaging [2, 10-13], sensing [9-11,13,14], catalysis [8,15,16] optoelectronics [17] and energy conversion [5,16,18]. In this work, we report the use of CNDs as an electrocatalyst support material in direct alcohol fuel cells. Direct alcohol fuel cells (DAFCs) are attractive as power sources, they employ low molecular weight cheap green fuels [19,20]. They have fascinating advantages such as high efficiency, high energy density [21], low working temperature [22], greatly simplified design [23] and quiet operation without vibration or noise. Ethanol is an attractive liquid fuel for sustainable energy systems since it is renewable [22,23,26] cheap and non-toxic [27]. Methanol, on the other hand, has been considered the most promising fuel because it is more efficiently oxidized than other alcohols. The challenges hindering the commercialization of DAFCs includes the poor alcohol electro-oxidation reaction kinetics [27,28], the poisoning effect of the anode catalysts by some intermediates, such as adsorbed CO [31-34] and the high cost of the platinum electrocatalyst [34,35]. These problems could be resolved by using nano-scale platinum, platinum alloys and/or platinum-free catalysts [38]. The activity of a catalyst for alcohol electro-oxidation depends on the particle size distribution and dispersion of catalyst and closely linked to the characteristics of the support used [4,39]. A good support material should have a high surface area which may be obtained through high porosity. It should also bond and interact with the electrocatalysts to improve the activity and durability of the metal nanoparticles [40]. In addition, the support material for a fuel cell catalyst must have sufficient electrical conductivity so that the support can act as a path for the flow of electrons [41]. Supporting electrolytes such as NaOH, KOH, H_2SO_4 or $HClO_4$ play a vital role in determining the overall fuel cell performance. Hence stability and corrosion resistance of the catalyst support material in fuel cell environment is of great importance in the development of new catalyst support materials [40,41]. Carbon black is widely used as a catalyst support. However, it easily gets corroded and gasified under the fuel cell environment resulting in agglomeration and detachment of platinum catalyst, this decreases the fuel cell performance

[42,43]. Carbon nanotubes have attracted much attention as catalyst support material in fuel cells. The challenge is that the pristine CNTs are chemically inert and are difficult to attach metal nanoparticles. For this reason, nanoparticles on CNTs have poor dispersion and large particle size, which diminishes the electrocatalytic activity. In order to overcome such difficulties, the surface of the pristine CNTs is usually modified using harsh acid for functionalization, which causes structural defects and reduces the electrical property of the modified CNTs surface [44,45].

In this work, a green and simple method for synthesizing carbon nanodots has been developed. We also present the use of carbon nanodots as a support material in direct alcohol fuel cells. Platinum nanoparticles were attached to the surface of carbon nanodots using water as a solvent in the absence of a surfactant or reducing agent without adjusting the pH of the solution. The oxygen functional

groups facilitated the attachment of catalyst nanoparticles on the surface of carbon nanodots. As expected, the Pt/CNDs electrocatalyst exhibited high electrocatalytic activity for alcohol oxidation (in acidic and alkaline electrolytes) compared to the commercial Pt/C.

2. EXPERIMENTAL

2.1. Material and Reagents

The following materials were used to prepare the electrocatalyst and electrolytes used in this study: Ethanol > 99.9% (Sigma-Aldrich), Methanol > 99.9% (Sigma-Aldrich), Nafion solution 20 wt.% (Sigma), H_2PtCl_6 98.0% (Sigma-Aldrich), H_2SO_4 95% (Sigma-Aldrich) and Sodium hydroxide pellets (Merck).

2.2. Instrumentation

Samples for TEM analysis were prepared by placing a drop of colloidal solution on the carbon-coated copper grid and then dried at room temperature. The size distribution of CNDs was performed by counting over 100 particles. XRD was performed on a Philips X-PertPro X-Ray Diffractometer using $\text{Cu K}\alpha$ radiation ($\lambda=0.154443$ nm, 40 mA and 40 kV). The surface functional groups and elemental states of CNDs were characterized by XPS (Kratos Axis Ultra DLD, using an Al (monochromatic) anode, equipped with charge neutralizer). XPS was also used to determine the oxidation states of platinum in Pt/CNDs electrocatalysts. FTIR was used to identify the functional groups present in CNDs. Platinum loading on CNDs was quantified using ICP-OES spectrometer (iCAP 6500 Duo, Thermo Scientific, UK). Calibration standards from 1-100 ppm were prepared from the platinum precursor. The sample for ICP-OES was prepared by digesting 25 mg of Pt/CNDs electrocatalyst in 4 mL of aqua regia, it was then diluted with ultrapure water to make 50 mL. The mixture was filtered to remove solids before analysis.

2.3 Synthesis of carbon nanodots

Carbon nanodots were synthesized according to a method reported by Shi et al [13] with modification. To describe the method briefly, 10 g of oats were weighed into a crucible and transferred into a muffle furnace and pyrolyzed at 400 °C for 2 hours. The black product was cooled to room temperature and then mechanically crushed to a fine powder. The powder was dispersed in ultrapure water and centrifuged several times to remove larger particles. The carbon nanodots aqueous suspension was filtered and the CNDs powder was obtained after drying in an oven at 80 °C for 24 hours.

2.4 Synthesis of Pt/CNDs electrocatalyst

The Pt/CNDs electrocatalyst was carried out as follows: CNDs were dispersed in ultrapure water and an appropriate amount of H_2PtCl_6 required to produce 10% wt Pt loading was added to the

CNDs aqueous suspension. The subsequent mixture was treated in an ultrasound bath for 30 minutes followed by reflux for 3 hours. The resulting suspension was filtered, washed several times with water to remove residual chloride and the solid was dried at 70 °C for 2 hours to obtain the Pt/CNDs electrocatalyst.

2.5 Electrochemical techniques

The working electrode was prepared by dispersing dry Pt/CNDs (10 mg) electrocatalyst in 2.5 mL ultrapure water containing 2 drops of Nafion solution. The mixture was treated in an ultrasound bath for 10 min forming a homogeneous ink. Five microliters of the ink were deposited onto the cavity of a clean pyrolytic graphite electrode (basal plane) and dried at room temperature. The electrode was polished using sandpaper and then sonicated with ultrapure water to remove loose particles from the sand paper. Voltammetric and chronoamperometric measurements were carried out using a Dropsens potentiostat. A Ag/AgCl (saturated with 3 M NaCl solution) was used as a reference and a platinum wire was used as a counter electrode. The commercial 10 %wt Pt/C electrocatalyst was prepared in a similar way and all electrochemical tests were done at room temperature. The electrolyte solutions were purged with argon gas for 30 minutes prior the experiment to eliminate oxygen.

3. RESULTS AND DISCUSSION

3.1 Characterization of nanoparticles

3.1.1 Transmission electron microscopy

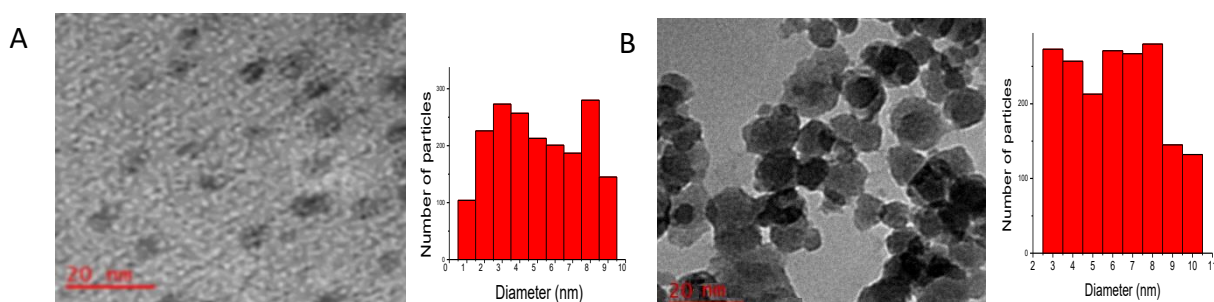


Figure 1. HRTEM images for (a) CNDs and (b) Pt/CNDs.

The TEM micrograph of the carbon nanodots shows that CNDs are monodispersed and exhibit spherical and oval shapes. It can be seen from the particle distribution histogram that the carbon nanodots synthesized with pyrolysis of oats have an average particle size of 4 nm. These were smaller than those reported by Shi et al [13]. Fig. 1b shows TEM image of Pt/CNDs electrocatalyst, the particle sizes increases from 4 nm to 7 nm after depositing platinum nanoparticles. It should be pointed that the average particle size for the electrocatalyst includes the size of carbon nanodots plus the size of platinum nanoparticles. Therefore, average particle size of the platinum nanoparticles was calculated to

be 2.1 nm from XRD peak of Pt (111) using Debye–Scherer equation; $D = k\lambda/\beta\cos\Theta$. The BET surface area of carbon nanodots was found to be $312.5 \text{ m}^2\text{g}^{-1}$ whereas the BET surface area of commercial activated carbon is $142.6 \text{ m}^2\text{g}^{-1}$. The pore volume of carbon nanodots was found to be $0.2 \text{ cm}^3\text{g}^{-1}$.

3.1.2 FTIR

FTIR study shows that oxygen-containing functional groups are present in the synthesized carbon nanodots. Vibrational peaks corresponding to -C-O, -C=O and -C-H can be seen in Fig. 2. The characteristic peak at 3422 cm^{-1} is attributed to the O-H stretching while the peak at 2850 cm^{-1} is assigned to the -C-H deformation of CH_2 . The peaks in the region of $1250\text{-}1320 \text{ cm}^{-1}$ correspond to the C-O stretching while the peaks in the region of $1400\text{-}1650\text{cm}^{-1}$ were assigned to the O=C-O functional group. The FTIR spectra indicate that the carboxyl functional group is the most dominant on the surface of the CNDs as reported by other researchers [5,7,11,13,18]. These functional groups facilitate attachment of metal nanoparticle on the surfaces of carbon nanodots [5].

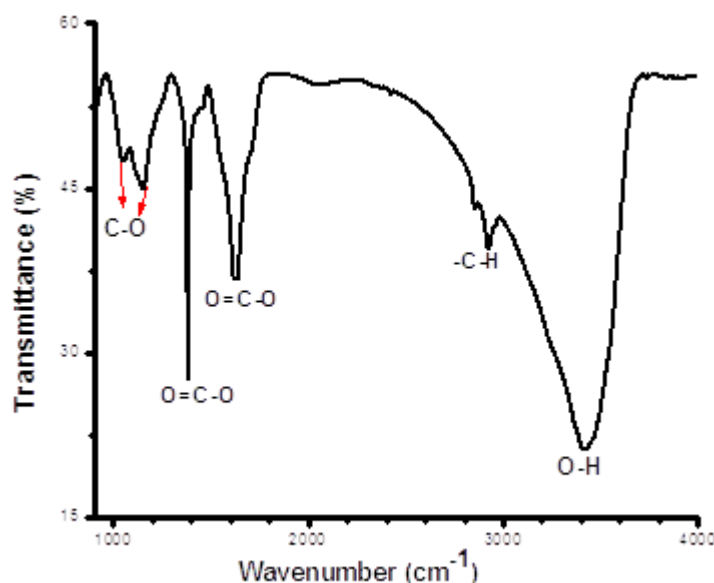


Figure 2. FTIR spectra for carbon nanodots.

3.1.3 X-ray photoelectron spectroscopy

X-ray photoelectron spectroscopy (XPS) is a powerful tool for revealing the electron structures and valence states of elements. XPS spectra revealed the presence of C-C, C=C, C-O and -C=O. Fig. 3a shows the XPS survey spectra of the synthesized materials in which O 1s, C 1s, N 1s, Pt 4f, a trace of Si 2p and Na 1s signals were detected. The major peaks were deconvoluted, C1s spectra for CNDs (Fig. 3b) shows five peaks. The peaks at 284.65 and 286.22 eV correspond to the binding energy of C-C/C=C and C-O bonds respectively while the peaks at 287.76, 289.66 and 292.29 eV are attributed to the carboxylic groups.

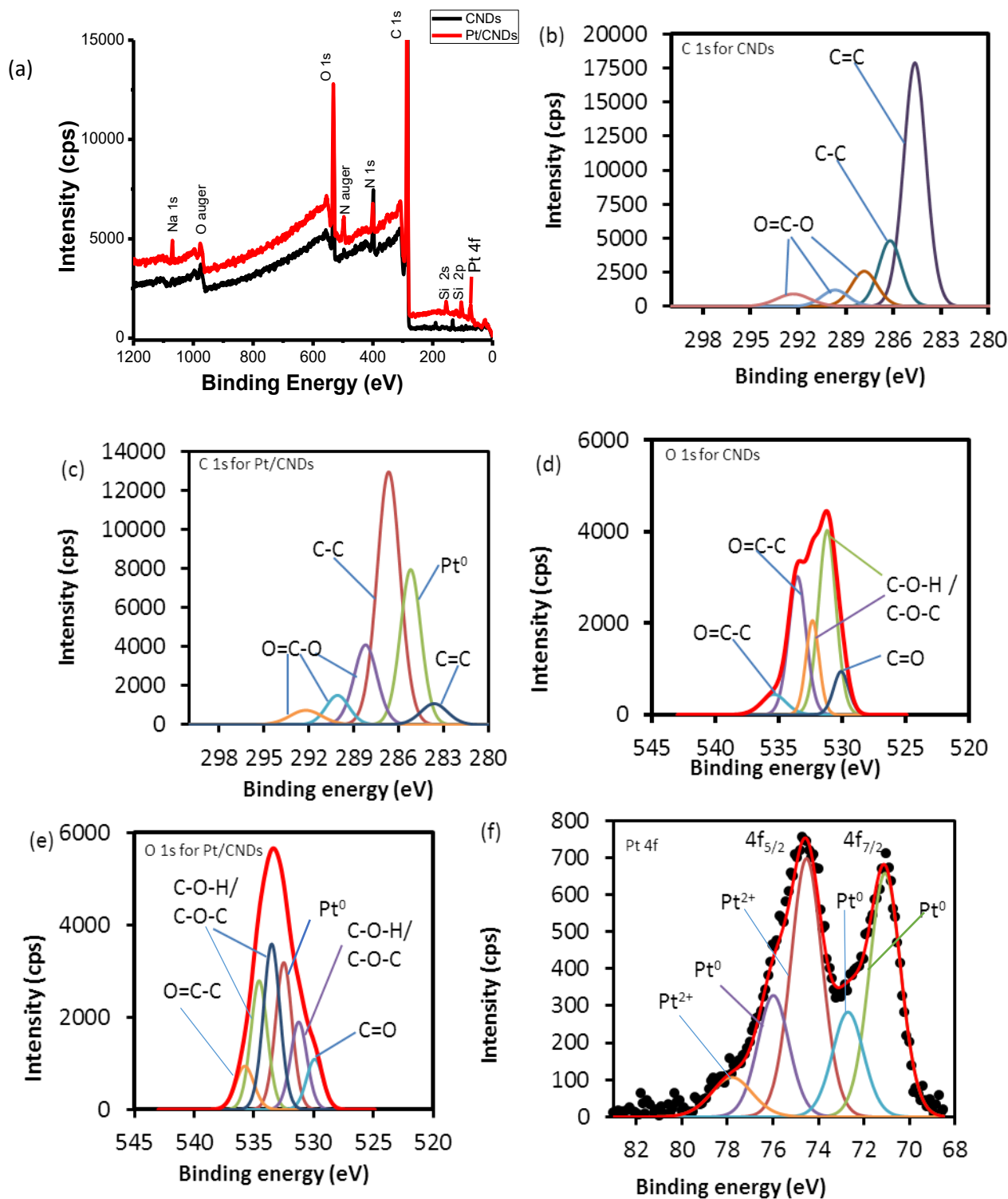


Figure 3. XPS (a) survey spectra for (b) C 1s of CNDs, (c) C 1s of Pt/CNDs, (d) O 1s of CNDs, (e) O 1s of Pt/CNDs, (f) Pt 4f spectra for Pt/CNDs electrocatalyst.

The O 1s spectrum for CNDs (Fig. 3d) shows two peaks at 530.07 and 531.20 eV which are ascribed to C=O and C-O-H/C-O-C respectively. The peaks at 532.34, 533.56 and 535.38 eV are assigned to the O-C=O functional group. The XPS results confirm that the synthesized CNDs are functionalized with carboxylic moieties [11,13]. These XPS data are in good agreement with the FTIR

analysis. Fig. 3(c, e and f) shows the XPS spectra of the Pt/CNDs electrocatalyst. The C 1s and O 1s XPS spectra for Pt/CNDs show the presence of six peaks. The addition of Pt leads to Pt-O (coordination) at Pt/CNDs composite. Platinum with an oxidation state of +2 was obtained implying that platinum was bonded to the support material at C-O-H or C-O-C. Two broad peaks were for Pt 4f spectra, these were due to Pt 4f_{7/2} and Pt 4f_{5/2} with splitting energy of 3.33 eV. Upon deconvolution five peaks were observed as shown in Fig. 3f, the peaks at 70.50, 71.12 and 74.41 eV were due to metallic platinum (Pt⁰) and Pt-O (Pt²⁺) was assigned to peaks at 72.95 and 76.19 eV [46]. The binding energies of the metallic platinum are in agreement with typical values reported in literature [46,47]

Table 1 shows the elemental composition of CNDs and Pt/CNDs, it can be seen that carbon nanodots are mainly composed of carbon, oxygen and nitrogen. This is because oats contain carbohydrates and proteins. XPS also revealed that Pt/CNDs electrocatalyst contains 8.23% platinum. ICP-OES results showed that 40.58 ppm of platinum was present in the Pt/CNDs electrocatalyst. Therefore, there was 2.03 mg platinum in 25 mg of the electrocatalyst that was digested and diluted to make 50 mL of the solution. Hence the platinum loading on CNDs was found to be 8.12%. This is slightly lower than 8.23% as determined by XPS, this may be due to incomplete digestion of the sample used for ICP-OES analysis. The Pt/CNDs electrocatalyst also contains traces of silicon and sodium, these may be coming from the platinum precursor (H₂PtCl₆) as impurities. The fraction of Pt and Pt-O species calculated from the relative intensities of deconvoluted peaks and Pt/CNDs surface composition observed from the XPS results are summarized in Table 1. Pt⁰ (60.23%) is the predominant species in the Pt/CNDs electrocatalyst implying that carbon nanodots are capable of reducing Pt⁴⁺ to Pt⁰. A significant amount of Pt-O (39.77%) was observed. These Pt-O species are important sites for CO oxidation [48].

Table 1. Elemental composition of CNDs and Pt/CNDs obtained from XPS data.

Sample	Na %	C %	O %	N %	Si %	Pt %
CNDs	-	82.31	9.64	8.04	-	-
Pt/CNDs	0.063	78.60	9.18	3.18	0.80	8.23 Pt ⁰ =60.23% Pt ²⁺ (Pt-O)=39.77%

Fig. 4 shows the XRD patterns of the synthesized carbon nanodots and Pt/CNDs electrocatalyst. The XRD pattern of carbon nanodots showed a broad peak centred at 24.2°. These results suggest that the synthesized carbon material was amorphous [5,49]. The pattern for Pt/CNDs showed intense diffraction peaks at 39.8°, 46.5° and 67.8°. These diffractions correspond to Pt (111), Pt (200) and Pt (220). Pt(111) has been found to be the most active facet for alcohol electro-oxidation with lower poisoning rates [50]. A strong diffraction peak was observed for Pt (111), this showed that the synthesized Pt/CNDs electrocatalyst is structurally promising to be an active electrocatalyst.

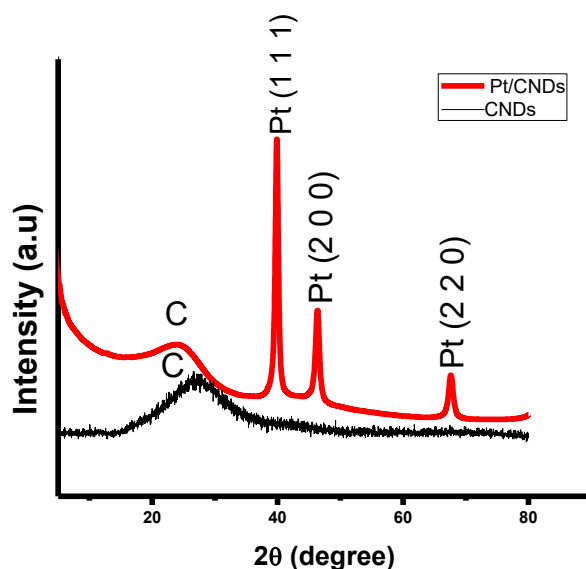


Figure 4: XRD patterns of the synthesized carbon nanodots and the Pt/CNDs electrocatalyst.

3.2 Application of electrocatalyst for methanol electro-oxidation

3.2.1 Cyclic Voltammetry

Fig. 5(a) and (b) show cyclic voltammograms for methanol electro-oxidation in both acidic and alkaline conditions. The methanol electro-oxidation reaction is characterized by two distinct forward and backward current peaks. The forward scan is attributed to methanol oxidation and the peak represents the electro-oxidation of freshly chemisorbed species resulting from adsorbed methanol. The backward scan peak corresponds to the removal of intermediates incompletely oxidized in the forward scan [51]. The size of the forward peak indicates the catalytic activity for the electro-oxidation reaction of methanol [52].

From Fig. 5(a) and (b) it can be seen that the electrocatalytic activity for methanol oxidation on platinum nanoparticles supported on carbon nanodots is higher than that of commercial platinum nanoparticles supported on activated carbon in both acidic and alkaline media. This may be due to the high surface area [53] and higher platinum utilization provided by the support material (carbon nanodots). It should be noted that with the same methanol concentration a higher current density was obtained under alkaline conditions at a relatively lower potential. This is because of faster methanol adsorption and the availability of oxygen-containing species (OH^-) in alkaline media [54].

The magnitude of the backward peak is less than that of the forward in alkaline medium, this is because the removal of adsorbed carbonaceous species is easier due to the availability of oxygen-containing species that facilitate quick methanol oxidation [54]. Large amounts of water are required in methanol oxidation reaction in acidic media to prevent partial methanol oxidation which produces intermediates that poison the platinum electrocatalyst, hence a lower methanol concentration was used [55].

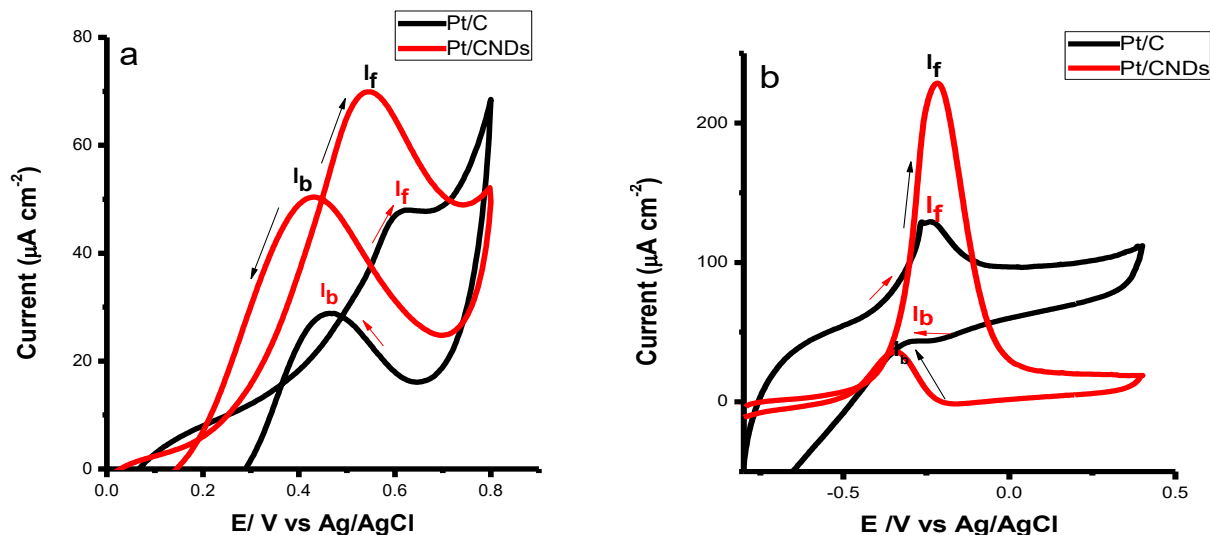


Figure 5. Cyclic voltammetry graphs for commercial Pt/C and Pt/CNDs in (a) 0.5 methanol in 0.5M H_2SO_4 , (b) 0.5M methanol in NaOH electrolyte at a scan rate of 50mV s^{-1} at room temperature.

3.2.2 Chronoamperometry

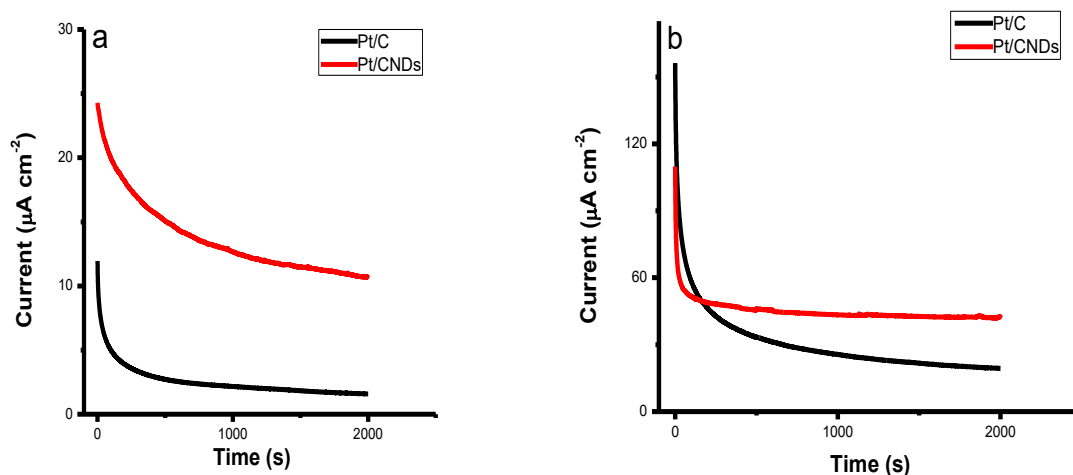


Figure 6: Chronoamperometric curves for Pt/C and Pt/CNDs (a) at 0.5V in 0.5 M methanol in 0.5 H_2SO_4 (b) at -0.2 V in 0.5M methanol + 0.5M NaOH electrolytes at room temperature.

Chronoamperometry is the best electrochemical method for studying the electrocatalyst poisoning rates. Fig. 6(a) and (b) shows chronoamperometry curves for the synthesized Pt/CNDs versus the commercial Pt/C in both acidic and alkaline conditions. In the beginning of the experiment a sharp current decay is observed especial in alkaline conditions, this is due to the formation of poisoning intermediates [38] such as CH_3OH (adsorbed), CHO , CO and CO_3^{2-} [54]. The chronoamperometry results showed that the synthesized Pt/CNDs electrocatalyst has lower poisoning rates compared to the commercial Pt/C for the entire period of 2000 seconds. It is noted that a steady current state was reached in shorter periods under alkaline conditions.

3.3 Application of electrocatalyst for ethanol electro-oxidation

3.3.1 Cyclic voltammetry

The cyclic voltammetry graphs for ethanol electro-oxidation in Fig. 7a show that the synthesized Pt/CNDs electrocatalyst yielded 2.1 times more current density compared to the commercial Pt/C. The ratio of the forward peak (I_f) to the backward peak (I_b) can be used to measure the degree of tolerance to poisoning caused by intermediates [51,56,57]. A larger ratio of (I_f/I_b) means improved catalytic activity. From the CV results it is observed that for the commercial Pt/C electrocatalyst the I_b is greater than I_f hence the ratio I_f/I_b is less than 0.85, this shows poor catalytic activity of the electrocatalyst. The synthesized electrocatalyst yielded a higher current density and the ratio (I_f/I_b) was 1.02. This shows that the synthesized platinum nanoparticles supported on carbon nanodots electrocatalyst exhibit a greater electrocatalytic activity for ethanol electro-oxidation in acidic media compared to the commercial Pt/C with 10% platinum loading. Ethanol electro-oxidation was conducted using 2M ethanol in 0.1M NaOH.

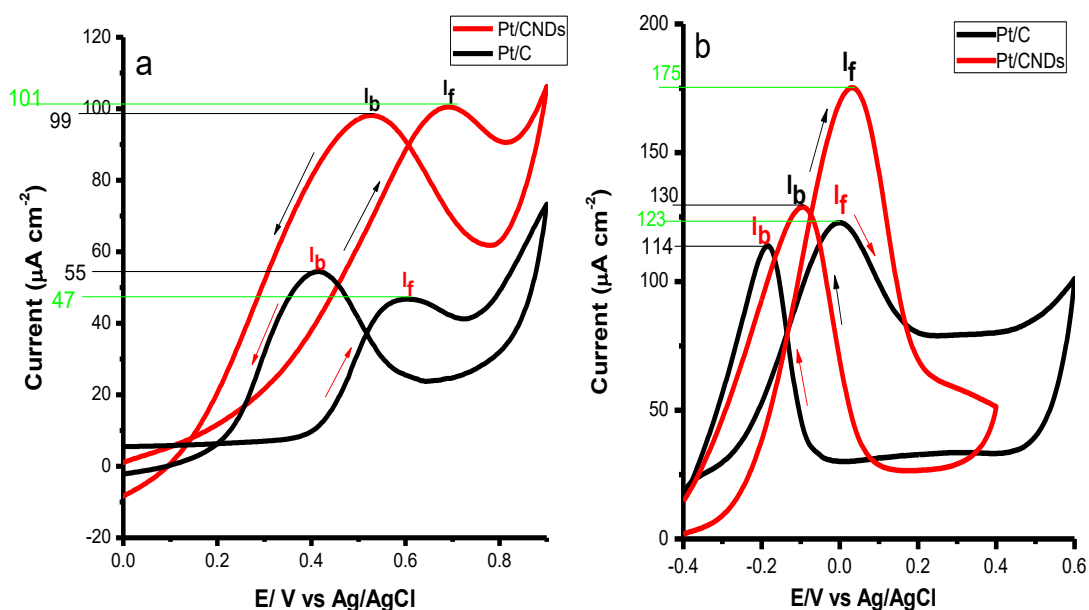


Figure 7. Cyclic voltammetry graphs for commercial Pt/C and Pt/CNDs in (a) 3M ethanol in 0.1M H_2SO_4 , (b) 2M ethanol in 0.1M NaOH electrolyte at a scan rate of 50mV s^{-1} at room temperature.

The CV curve is shown in Fig. 7b. The synthesized Pt/CNDs electrocatalyst yielded a higher current density compared to the commercial Pt/C. It is known that current density increases with ethanol concentration [35,40,58]. It is noted from cyclic voltammetry graphs that the synthesized electrocatalyst yields higher current densities ($175 \mu\text{A cm}^{-2}$) in alkaline media compared to acidic media ($101 \mu\text{A cm}^{-2}$ in 3M ethanol in H_2SO_4) with higher ethanol concentration. This implies that alkaline media is favourable for ethanol electro-oxidation. It has been reported that ethanol electro-oxidation kinetics are improved in alkaline conditions [21,60,61]. Higher current densities in alkaline media were also observed by Brouzguo et al. [62] and Zhao [58]. Enhanced activity in alkaline media

results from the lack of specifically adsorbing spectator ions and the higher OH coverage at lower potentials which is required for alcohol oxidation [19,63].

3.3.2 Chronoamperometry

Fig. 8(a) and (b) show chronoamperometry curves for ethanol electro-oxidation in both acidic and alkaline media. From chronoamperometry curves, it can be seen that both initial and steady-state oxidation current densities at Pt/CNDs electrode are much larger than those from commercial one over the entire period of 2000 seconds. A sharp current decrease is also observed at the beginning of reaction which is due to the formation of intermediates such $\text{CH}_3\text{CH}_2\text{OH}$ (adsorbed), CH_3CHO , CH_3COO^- , CH_4 and CO_3^{2-} which poison the platinum electrocatalyst.

The results show that the current density decay of the synthesized Pt/CNDs electrocatalyst is slower than that of Pt/C. Hence the synthesized electrocatalyst show a lower poisoning rate compared to the commercial Pt/C.

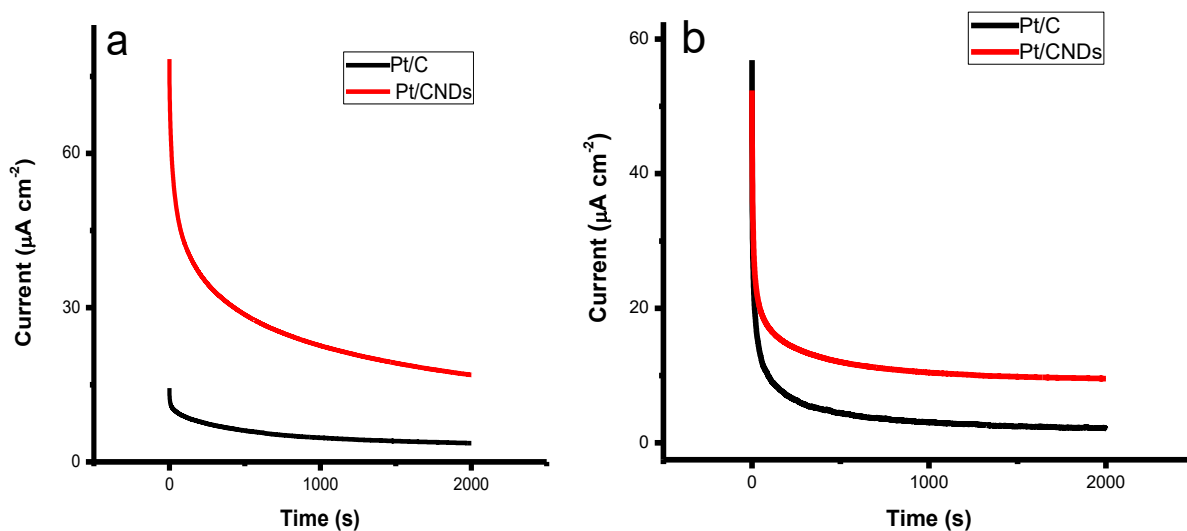


Figure 8. Chronoamperometric curves for Pt/C and Pt/CNDs (a) at 0.6V in 3 M ethanol in 0.1M H_2SO_4 (b) at 0.02 V in 2M ethanol + 0.1 M NaOH electrolytes at room temperature.

Table 2 compares the onset potentials (E_s) and peak potentials (E_p) for the synthesized Pt/CNDs electrocatalyst against other anode catalysts that have been studied. Lower onset potentials indicate the easiness of the oxidation reaction due to improved kinetics; hence an electrocatalyst with low onset and peak potentials is regarded as a better anode catalyst.

From Table 2 it can be seen that the onset potential for the synthesized Pt/CNDs is lower than that of Pt/CNTs for ethanol and methanol oxidation in acidic media. In alkaline media it is observed that the Pt/CNDs electrocatalyst shows superior performance against Pt/ Vulcan carbon XC-72 and Pd/ Vulcan carbon XC-72 for alcohol oxidation. The results also show that palladium supported on carbon nanotubes (Pd/CNTs) and palladium supported on nitrogen doped graphene (Pd/NGN) have lower onset potentials compared to the synthesized Pt/CNDs electrocatalyst in alkaline media. It has been reported that Pd performs better than platinum in alkaline conditions [64]. The table also shows that

the Pt/CNDs electrocatalyst performs better than the Pt/ Vulcan carbon XC-72 in acidic media. The results prove that the synthesized Pt/CNDs electrocatalyst can be potentially applied in acidic direct alcohol fuel cells.

Table 2. Comparison of electrochemical performance of Pt/CNDs against other anode catalysts for direct alcohol fuel cells.

Electrocatalyst	Ethanol				Methanol				Ref
	Es /V acidic	Es /V alkaline	Ep /V acidic	Ep /V alkaline	Es /V acidic	Es /V alkaline	Ep /V acidic	Ep /V alkaline	
Pt/C	0.17	-0.31	0.60	0.021	0.35	-0.40	0.52	-0.24	
Pt/CNDS	0.21	-0.22	0.69	0.035	0.27	-0.41	0.61	-0.21	This work
Pt/CNTs	0.60	-0.60	0.80	-0.10	0.65	-0.58	0.85	-0.10	[65,66]
Pd/CNTs	–	-0.62	–	-0.22	–	-0.45	–	-0.20	[65,66]
Pt/ Vulcan carbon XC-72	0.70	0.45	0.98	0.90	0.55	0.60	0.85	0.85	[67,68]
Pd/ Vulcan Carbon XC-72	–	0.45	–	0.95	–	-0.30	–	-0.18	[67,68]
Pd/ NGN	–	-0.60	–	-0.20	–	-0.55	–	-0.15	[64]
Pt/ NGN	–	-0.58	–	-0.10	–	-0.58	–	-0.12	[64]

4. CONCLUSION

Highly functionalized carbon nanodots were successfully synthesized using a simple and cheap method. Surface characterization techniques proved that platinum nanoparticles can be attached to the surface of CNDs through oxygen functional groups. Electrochemical tests showed that the synthesized Pt/CNDs electrocatalyst exhibit greater activity for alcohol electro-oxidation compared to the commercial Pt/C in both acidic and alkaline conditions. Methanol electro-oxidation in alkaline media yielded the highest current density. Chronoamperometry results show that the Pt/C electrocatalyst current density decay is rapid compared to that of the synthesized Pt/CNDs electrocatalyst.

ACKNOWLEDGEMENTS

The authors are grateful to the University of Johannesburg, Faculty of Science, University Research Council, Centre for Nanomaterials Science Research and National Research Foundation (TTK-15071-0125-019) for the financial support.

References

1. S. N Baker and G. N Baker, *Ang. Chem. Int. Ed.*, 49 (2010) 6726.

2. H. Li, Z. Kang, Y. Liu and S.T. Lee, *J. Mater. Chem.*, 22 (2012) 24230.
3. P. Roy, P. C. Chen, A. P. Periasamy, Y. N. Chen and H. T. Chang, *Mater. Today*, 18 (2015) 447.
4. S. Zhu, Y. Song, X. Zhao, J. Shao, J. Zhang and B. Yang, *Nano Res.*, 8 (2015) 355.
5. W. Wei and W. Chen, *J. Power Sources*, 204 (2012) 85.
6. X. Qin, W. Lu, A. M. Asiri, A. O. Al-Youbi and X. Sun, *Sensors Actuators, B Chem.*, 184 (2013) 156.
7. R. S. A. Sonthanasamy, W. Y. W. Ahmad, S. Fazry, N. I. Hassan and A. M. Lazim, *Carbohydr. Polym.*, 137 (2016) 488.
8. F. Yan, D. Kong, Y. Fu, Q. Ye, Y. Wang and L. Chen, *J. Colloid and Interface Sci.*, 466 (2016) 268.
9. L. Shi, Y. Li, X. Li, B. Zhao, X. Wen, G. Zhang, C. Dong and S. Shuang, *Biosens. Bioelectron.*, 77 (2016) 598.
10. J. Zhang and S. H. Yu, *Mater. Today*, (2015) 1.
11. X. Wen, L. Shi, G. Wen, Y. Li, C. Dong, J. Yang and S. Shuang, *Sensors Actuators, B Chem.*, 221 (2015) 769.
12. X. T. Zheng, A. Ananthanarayanan, K. Q. Luo and P. Chen, *Small*, 11 (2015) 1620.
13. L. Shi, X. Li, Y. Li, X. Wen, J. Li, M. M. F. Choi, C. Dong and S. Shuang, *Sensors Actuators, B Chem.*, 210 (2015) 533.
14. Z. Luo, X. Ma, D. Yang, L. Yuwen, X. Zhu, L. Weng and L. Wang, *Carbon N.Y.*, 57 (2013) 470.
15. H. Zhang, J. Chen, Y. Li, P. Liu, Y. Wang, T. An and H. Zhao, *Electrochim. Acta*, 165 (2015) 7.
16. Z. Y. Shih, A. P. Periasamy, P. C. Hsu and H. T. Chang, *Appl. Catal. B. Environ.*, 132 (2013) 363.
17. L. Wang, S. Zhu, H. Wang, S. Qu, Y. Zhang, J. Zhang and Q. Chen, *ACS.*, 3 (2014) 2541.
18. A. Biswas, S. Paul and A. Banerjee, *J. Mater. Chem. A*, 3 (2015) 15074.
19. Z. J. Mellinger and J. G. Chen, *Electrocatalysis in Fuel Cells*, 9 (2013) 197.
20. B. Habibi and S. Mohammadyari, *Int. J. Hydrogen Energy*, 40 (2015) 10833.
21. E. Antolini and E. R. Gonzalez, *J. Power Sources*, 195 (2010) 3431.
22. K. Charoen, C. Prapainainar, P. Sureeyatanapas, T. Suwannaphisit, K. Wongamornpitak, P. Kongkachuichay, S. M. Holmes and P. Prapainainar, *J. Clean. Prod.*, (2016) 85.
23. A. Lavacchi, H. Miller and F. Vizza, Springer (2013), Sesto Fiorentino, Italy.
24. Y. Xu and B. Zhang, *Chem, Society reviews*, 43 (2014) 2439.
25. B. Liu, Z. W. Chia, Z. Y. Lee, C. H. Cheng, J. Y. Lee and Z. L. Liu, *Fuel Cells*, 12 (2012) 670.
26. S. Meenakshi, K. G. Nishanth, P. Sridhar and S. Pitchumani, *Electrochim. Acta*, 135 (2015) 52.
27. A. Sayadi and P. G. Pickup, *Electrochim Acta*, 215 (2016) 84.
28. E. V. Spinacé, R. R. Dias, M. Brandalise, M. Linardi and A. O. Neto, *Ionics*, 16 (2010) 91.
29. M. Chen, B. Lou, Z. Ni and B. Xu, *Electrochim. Acta*, 165(2015) 105.
30. K. I. Ozoemena, *RSC Adv.*, 6 (2016) 89523.
31. I. Choi, S. H. Ahn, M. H. Kim, O. J. Kwon and J. J. Kim, *Int. J. Hydrogen Energy*, 39 (2014) 3681.
32. S. Balasubramanian, B. Lakshmanan, C. E. Hetzke, V. A. Sethuraman and J. W. Weidner, *Electrochim. Acta*, 58 (2011) 723.
33. S. M. Kim, L. Liu, S. H. Cho, H. Y. Jang and S. Park, *J. Mater. Chem. A*, 48 (2013) 15252.
34. A. Arun, M. Gowdhamamoorthi, K. Ponmani, S. Kiruthika, and B. Muthukumar, *RSC Adv.*, 5 (2015) 49643.
35. L. Han, H. Ju and Y. Xu, *Int. J. Hydrogen Energy*, 37 (2012) 15156.
36. L. D. Zhu, T. S. Zhao, J. B. Xu and Z. X. Liang, *J. Power Sources*, 187 (2009) 80.
37. R. Liang, A. Hu, J. Persic and Y. N. Zhou, *Nano-Micro Lett.*, 5 (2013) 202.
38. T. G. H. Nguyen, T. V. A. Pham, T. X. Phuong, T. X. B. Lam, V. M. Tran and T. P. T. Nguyen, *Ad. Nat. Sci. Nanosci. Nanotechnol.*, 4 (2013) 35008.
39. J. Goel and S. Basu, *Int. J. Hydrogen Energy*, 39 (2014) 15956.
40. A. L. Dicks, *J. Power Sources*, 156 (2006) 128.

41. E. Antolini and E. R. Gonzalez, *Appl. Catal. A Gen.*, 365 (2009) 1.
42. J. Liu, C.T. Liu, L. Zhao, J. J. Zhang, L. M. Zhang and Z.B. Wang, *Int. J. Hydrogen Energy*, 41 (2015) 1859.
43. Z. Z. Jiang, Z. B. Wang, Y. Y. Chu, D. M. Gu and G. P. Yin, *Energy Environ. Sci.*, 4 (2011) 2558.
44. D. Prasanna and V. Selvaraj, *RSC Adv.*, 5 (2015) 98822.
45. P. Trogadas, T. F. Fuller and P. Strasser, "Carbon as catalyst and support for electrochemical energy conversion," *Carbon N.Y.*, 75 (2014) 5.
46. F. E. Lopez-Suarez, C. T. Carvalho-Filho, A. Bueno-Lopez, J. Arboleda, A. Echavarria, K. I. B. Eguiluz and G. R. Salazar-Banda, *Int. J. Hydrogen Energy*, 40 (2015) 12674.
47. T. Lopes, E. Antolini and E. R. Gonzalez, *Int. J. Hydrogen Energy*, 33 (2008) 5563.
48. M. N. Tom Zawodzinski, Andrzej Wieckowski, Sanjeev Mukerjee and Matt Neurock, *Electrochem. Soc. Int.*, (2007) 37.
49. S. F. Chin, S. N. A. M. Yazid, S. C. Pang and S. M. Ng, *Mater. Lett.*, 85 (2012) 50.
50. E. Teliz, V. Díaz, R. Faccio, W. Mombrú and C. F. Zinola, *Int. J. Electrochem.*, 2011 (2011) 1.
51. X. Xiao, D. Huang, Y. Luo, M. Li, M. Wang and Y. Shen, *RSC Adv.*, 6 (2016) 100437.
52. C. Xu, Y. Liu and D. Yuan, *Int. J. Electrochem.Sci.*, 2 (2007) 674.
53. C. Xu, L. Cheng, P. Shen and Y. Liu, *Electrochem.commun.*, 9 (2007) 997.
54. M. Jing, L. Jiang, B. Yi and G. Sun, *J. Electroanal. Chem.*, 688 (2013) 172.
55. A. Alipour, S. Rowshanzamir and M. Javad, *Energy*, 94 (2016) 589.
56. A. M. Hofstead-Duffy, D. J. Chen, S. G. Sun and Y. J. Tong, *J. Mater.Chem.*, 22 (2012) 5205.
57. D. Y. Chung, K. J. Lee and Y. E. Sung, *J. Phys.Chem C*, 120 (2016) 9028.
58. L. An and T. S. Zhao, *Int. J. Hydrogen Energy*, 36 (2011) 9994.
59. L. An, Z. H. Chai, L. Zeng, P. Tan and T. S. Zhao, *Int. J. Hydrogen Energy*, 38 (2013) 14067.
60. S. Abdullah, S. K. Kamarudin, U. A. Hasran, M. S. Masdar and W. R. W. Daud, *J. Power Sources*, 320 (2016) 111.
61. W. W. Yang, M. Y. Lu and Y. L. He, *Int. J. Hydrogen Energy*, (2016) 1.
62. A. Brouzgou, A. Podias and P. Tsiakaras, *J. Appl. Electrochem.*, 43 (2013) 119.
63. A. M. Sheikh, K. E. A. Abd-Alftah and C. F. Malfatti, *J. Multidiscip.Eng. Sci.Technol.*, 1 (2014) 1.
64. J. Wang, N. Cheng, M. N. Banis, B. Xiao, A. Riese and X. Sun, *Electrochim. Acta*, 185 (2015) 267.
65. G. Yang, Y. Zhou, H. Bin Pan, C. Zhu, S. Fu, C. M. Wai, D. Du, J. J. Zhu and Y. Lin, *Ultrasonics Sonochemistry*, 28 (2016) 192.
66. Z. I. Bedolla-Valdez, Y. Verde-Gomez, A. M. Valenzuela-Muniz, Y. Gochi-Ponce, M. T. Oropeza-Guzman, G. Berhault and G. Alonso-Nunez, *Electrochim. Acta*, 186 (2015) 76.
67. Y. Tang, F. Gao, S. Mu, S. Yu and Y. Zhao, *Russ. J. Electrochem.*, 51 (2015) 345.
68. L. Ma, D. Chu and R. Chen, *Int. J. Hydrogen Energy*, 37 (2012) 11185.